Palaeogeography, Palaeoclimatology, Palaeoecology 311 (2011) 215–223

Contents lists available at SciVerse ScienceDirect

Palaeogeography, Palaeoclimatology, Palaeoecology

journal homepage: www.elsevier.com/locate/palaeo

Reconstructions of late Holocene paleofloods and glacier length changes in the Upper Engadine, Switzerland (ca. 1450 BC–AD 420)

Monique M. Stewart [a,*], Martin Grosjean [a], Franz G. Kuglitsch [a], Samuel U. Nussbaumer [b], Lucien von Gunten [a]

[a] Institute of Geography and Oeschger Centre for Climate Change Research, University of Bern, Bern, Switzerland
[b] Department of Geography, University of Zurich, Zürich, Switzerland

ARTICLE INFO

Article history:
Received 19 December 2010
Received in revised form 18 August 2011
Accepted 30 August 2011
Available online 7 September 2011

Keywords:
Lake sediments
Climate change
Alps
Floods
Glacier advances
Holocene

ABSTRACT

The relationship between summer-autumn floods in Central Europe and climate warming is poorly constrained by available instrumental, historical, proxy and model data. To investigate this relationship, a complete record of paleofloods, regional glacier length changes (and associated climate phases) and regional glacier advances and retreats (and associated climate transitions) are derived from the varved sediments of Lake Silvaplana (ca. 1450 BC–AD 420; Upper Engadine, Switzerland). In combination, these records provide insight into the behavior of floods (i.e. frequency) under a wide range of climate conditions.

Eighty-five paleofloods are identified from turbidites in the sediments of Lake Silvaplana. Regional glacier length changes (and associated cool and/or wet and warm and/or dry climate phases) are inferred from centennial anomalies in the square root of low-pass (LP) filtered Mass Accumulation Rates ($MAR_{LP}^{1/2}$). Regional glacier advances and retreats (and associated cooling and/or wetting and warming and/or drying climate transitions) are inferred from centennial trends in MAR_{LP}. This is the first continuous record of glacier length changes in the Lake Silvaplana catchment for this time period. These data agree with regional records of land-use, glacier activity and lake levels.

More frequent turbidites are found during cool and/or wet phases of ca. 1450 BC to AD 420. However, no relationship to climate transitions is discerned. Consistently, June–July–August (JJA) temperatures dating ca. 570 BC–AD 120 are inversely correlated to the frequency of turbidites. The rate that turbidite frequency increases with cooler JJA temperatures is not linear. Finally, 130 analogues for a 21st century climate in the Alps between ca. 570 BC–AD 120 (i.e. 50 year windows with a warming trend and average JJA temperature exceeding AD 1950–AD 2000 values from nearby meteo station Sils Maria) are considered. These reveal that turbidites are less frequent than between ca. 1450 BC–AD 420.

© 2011 Elsevier B.V. All rights reserved.

1. Introduction

Regional climate models project that future climate warming in Central Europe will bring more intense summer-autumn heavy precipitation and floods as the atmospheric concentration of water vapor increases and cyclones intensify (Arnell and Liu, 2001; Christensen and Christensen, 2003; Kundzewicz et al., 2005). This is relevant because recent flood events have cost human lives and damaged infrastructure (Brázdil et al., 2002; Trenberth et al., 2007). However, the relationship between climate warming and floods (i.e. frequency) is poorly constrained by instrumental data, historical data, natural proxies and climate models (e.g. Brázdil et al., 2002; Mudelsee et al., 2003, 2004; Pauling et al., 2006; Pfister et al., 2006; Caviezel, 2007; Gimmi et al., 2007; Debret et al., 2010; Schmocker-Fackel and Naef, 2010). In this article we show that the sediments of Lake Silvaplana can provide insight into the relationship between floods (i.e. frequency) and climate (i.e. cool and/or wet phases, warm and/or dry phases, cooling and/or wetting climate transitions and warming and/or drying climate transitions).

Floods enhance the discharge of rivers and mobilize large sediment loads (Gilbert and Desloges, 1987; Desloges and Gilbert, 1994; Knighton, 1998). Where these rivers enter lakes, turbidites can form. Therefore, the frequency of turbidites should be a reliable proxy for the frequency of paleofloods, extreme summer-autumn precipitation and the associated synoptic-scale meteorological situation.

In addition to reconstructing intense summer–autumn precipitation and floods, the sediments of Lake Silvaplana can provide insight into past climate phases. The square root of low frequency (100 year low-pass filtered, LP) changes in Mass Accumulation Rates ($MAR_{LP}^{1/2}$) are closely related to glacier lengths in the catchment (Leemann and Niessen, 1994; Ohlendorf et al., 1997; Blass et al., 2007; Nussbaumer et al., 2011). Because glacier length changes are mainly driven by

* Corresponding author. Tel.: +41 31 631 5092.
E-mail address: stewart@giub.unibe.ch (M.M. Stewart).

0031-0182/$ – see front matter © 2011 Elsevier B.V. All rights reserved.
doi:10.1016/j.palaeo.2011.08.022

long-term changes in climate (e.g. Steiner et al., 2005), $MAR_{LP}^{1/2}$ provides an approximation of cool and/or wet phases (positive anomalies of $MAR_{LP}^{1/2}$), warm and/or dry phases (negative anomalies of $MAR_{LP}^{1/2}$), cooling and/or wetting climate transitions (positive linear trends of $MAR_{LP}^{1/2}$) and warming and/or drying climate transitions (negative linear trends of $MAR_{LP}^{1/2}$).

Finally, Biogenic Silica (BSi) flux and chironomids in the sediments of Lake Silvaplana were successfully used to reconstruct June–July–August (JJA) temperatures for the last millennium (Trachsel et al., 2010) and from 570 BC–AD 120 (including the local expression of the Iron Age and Roman Period; Stewart et al., 2011).

Lake Silvaplana is an ideal archive to study paleofloods and climate phases because it has annually laminated (i.e. varved) sediments for the last 3300 years except for episodic turbidites (Leemann and Niessen, 1994). This provides an approximately annual chronology. Furthermore, the relationship between Lake Silvaplana sediments from the last millennium, floods, glacier activity, and summer temperatures is understood through previous studies (e.g. Leemann and Niessen, 1994; Ohlendorf, 1999; Blass, 2006; Trachsel et al., 2008; Nussbaumer et al., 2011). For the present study, the time window ca. 1450 BC to AD 420 was chosen because in Central Europe it contains greater interannual JJA temperature variability than the last millennium and includes prolonged windows which are warmer than expected for the 21st century (Stewart et al., 2011). Therefore, it can provide information about floods under a broad range of natural climate variability including multiple analogues for a warmer 21st century.

This paper aims to address the following questions: (1) What was the influence of long-term climate on turbidite frequency in the sediments of Lake Silvaplana between ca. 1450 BC and AD 420? (2) What was the influence of JJA temperatures on turbidite frequency in the sediments of Lake Silvaplana between ca. 570 BC and AD 120 (i.e. the years for which quantitative reconstructed JJA temperatures are available; Stewart et al., 2011)? (3) During windows with a trend and mean JJA temperature exceeding AD 1950–AD 2000 (i.e. analogues for the warmer 21st century), is turbidite frequency enhanced in the sediments of Lake Silvaplana?

2. Study area

Lake Silvaplana (1791 m a.s.l., between 46° 24′ N, 9° 42′ E and 46° 30′ N, 9° 52′ E) is located in the Upper Engadine valley of eastern Switzerland between lakes Sils and Champfèr. Lake Silvaplana has a surface area of 2.7 km^2, a volume of 127×10^6 m^3 and a mean depth of 47 m (Fig. 1; LIMNEX, 1994). Turnover occurs in May and November, stratification lasts from June to October and inverse thermal stratification (below ice cover) persists from January to May (LIMNEX, 1994; Ohlendorf, 1999).

The catchment (175 km^2) is underlain by three major tectonic nappes: the Lower Austroalpine Margna, the Upper Penninic Platta and the Lower Austroalpine Bernina consisting of granite, gneiss and carbonate (AdS, 2004; Blass, 2006). As of 1999, 5% of the catchment was glacier-covered (Kääb et al., 2002; Paul et al., 2002; Paul, 2007).

Lake Silvaplana is connected to the catchment by the Inn, Fedacla, Valhun and Surlej rivers (Blass, 2006). Inflowing water has an average residence time of eight months (LIMNEX, 1994).

A continental summer-dry climate dominates the region (Ohlendorf, 1999). In winter, temperature inversions favor the accumulation of cool and dry air in the Engadine valley, resulting in January to May ice-cover on the lake (Ohlendorf, 1999; MeteoSchweiz, 2010). Southerly moist air flow from over the Maloja Pass results in humid summers (Ohlendorf, 1999; MeteoSchweiz, 2010).

This climate favors larch (*Larix decidua*) and stone pine (*Pinus cembra*) vegetation in the catchment. Current tree-line (the elevation supporting trees>5 m tall) lies at 2410 m a.s.l. (Gobet et al., 2003). This region has sustained sporadic human settlements since the Mesolithic (e.g. artifacts from Valle Mesolcina date to 4850 BC). During

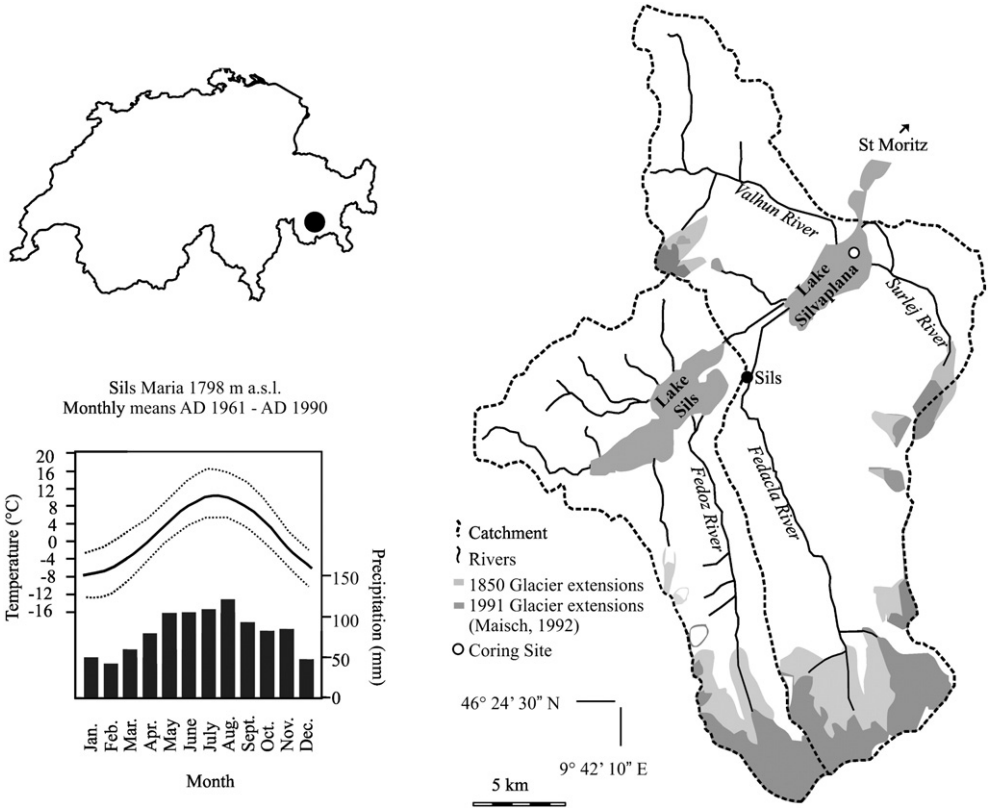

Fig. 1. The Lake Silvaplana catchment including major fluvial systems, glacier cover and mean temperature and precipitation (Sils Maria; 1961–1990) (Mappad Free Software, 1996; Blass, 2006; MeteoSchweiz, 2010). Data from Maisch, 1992.

the Bronze Age, copper prospecting expanded settlements near the Upper Engadine (e.g. Oberhalbstein). By the Iron and Roman Age, active trading across Alpine passes brought settlements to the Lower Engadine (Gobet et al., 2003).

3. Methods

3.1. Sampling

The lower six meters of a nine-meter UWITEC piston core (recovered from the ice in winter, 2005) were investigated. The core was cut lengthwise and photographed (2300×1700 pixels). Half of the core was wrapped in polyethylene film and stored at 4 °C until preparation of sediment blocks. The other half was flash-frozen with liquid nitrogen, covered in polyethylene film and preserved at −10 °C until subsampling.

3.2. Dating

A turbidite with an erosive basal surface at 3 m sediment depth (ca. AD 1177) prevented continuation of the varve chronology established for AD 1177–AD 2000 (Trachsel et al., 2010; Stewart et al., 2011). Three series of varve counts on resin impregnated and polished sediment blocks were used to develop a floating varve chronology. Varves could not be found below 6 m sediment depth. Therefore, only sediments from 3 m to 6 m were considered for the present study. For details regarding the construction of the polished sediment blocks the reader is directed to Stewart et al. (2011).

The three varve counts were combined with calibrated AMS radiocarbon dates (Poznań Radiocarbon Laboratory, Poland). Four radiocarbon dates from the total (mostly aquatic) organic carbon in bulk sediments (the upper sediment core; M. Trachsel, unpublished data) were subject to reservoir effects and consistently provided excessively old ages (i.e. ca. 4000 BC–7000 BC; inset, Fig. 2). This is likely related to carbonate bedrock in the catchment (Ohlendorf, 1999). Six radiocarbon dates were derived from small terrestrial macrofossils (e.g. twigs). Turbidites were the only location where terrestrial macrofossils could be found and these materials could be reworked. Therefore, the radiocarbon dates from the terrestrial macrofossils are interpreted as maximum ages. To estimate the degree of reworking, the difference in calibrated radiocarbon dates and in floating varve counts from consecutive terrestrial macrofossils was evaluated.

Following calibration of the radiocarbon dates in Intcal04.14 (Reimer et al., 2004), the three varve chronologies were fit through a turbidite at ~4.4 m depth. The varve chronology which minimized the difference between varve counts and ±2σ error radiocarbon years is the final chronology. Therefore, all ages presented here are calculated from an annually resolved floating varve chronology anchored by calibrated radiocarbon dates (BC and AD). For more details, the reader is directed to Stewart et al. (2011).

3.3. Sedimentological analyses

Mass Accumulation Rate (MAR) was calculated from varve thickness, dry sediment density and porosity. The dry sediment density was estimated at 2.65 g/cm^3 (= quartz) based on the geology of the catchment. Porosity was determined from the water content, dry sediment density and pore water density (ca. 1 g/cm^3; Blass et al., 2007). The thickness of laminations was measured on the high-resolution (1200 dpi) scans of the polished sediment blocks with Image-J software (Abramoff et al., 2004). Laminations exceeding 2σ of average varve thickness and/or having coarser grainsizes than surrounding sediments were interpreted as possible turbidites and excluded from MAR and varve counts.

3.4. Statistical analyses

Glacier length was reconstructed from the square root of 100 year Loess low-pass filtered MAR ($MAR_{LP}^{1/2}$) (Nussbaumer et al., 2011). The low-pass filter was set to a 100 year span to account for the time it takes larger glaciers (e.g. the Grosser Aletschgletscher) to respond to long-term climate changes (i.e. temperature and/or precipitation). The square root enabled comparison of glacier length changes (one-dimensional) to MAR (two-dimensional; for additional details consult Nussbaumer et al., 2011). Centennial anomalies (the difference between the 100 year average $MAR_{LP}^{1/2}$ and the record average) were

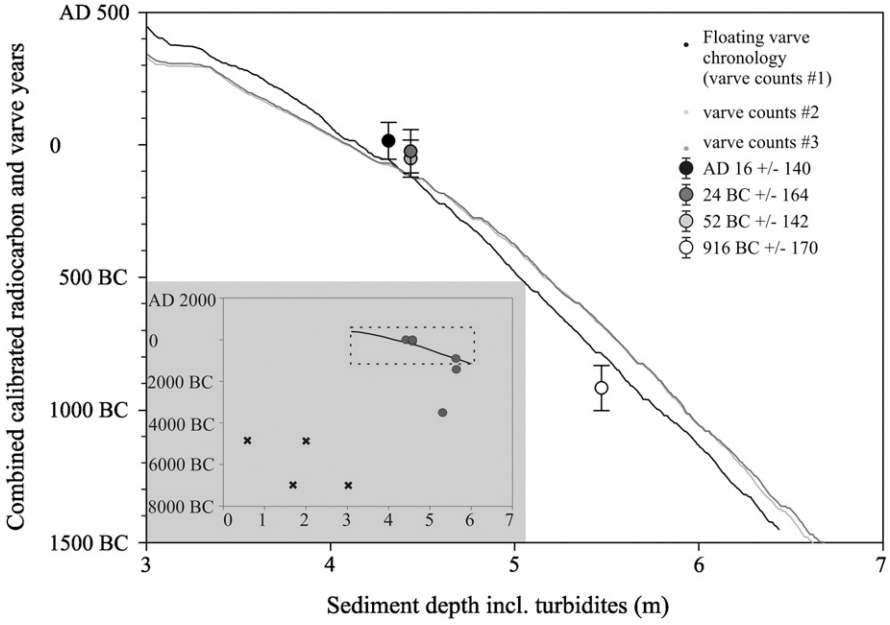

Fig. 2. The age-depth model including the three series of varve counts and the four elected calibrated AMS radiocarbon dates with error bars denoting two standard deviations. The inset provides the complete record of calibrated radiocarbon ages. Circles represent terrestrial macrofossil-derived radiocarbon dates whereas black crosses signify the bulk sediment-derived radiocarbon dates (M. Trachsel, unpublished data).

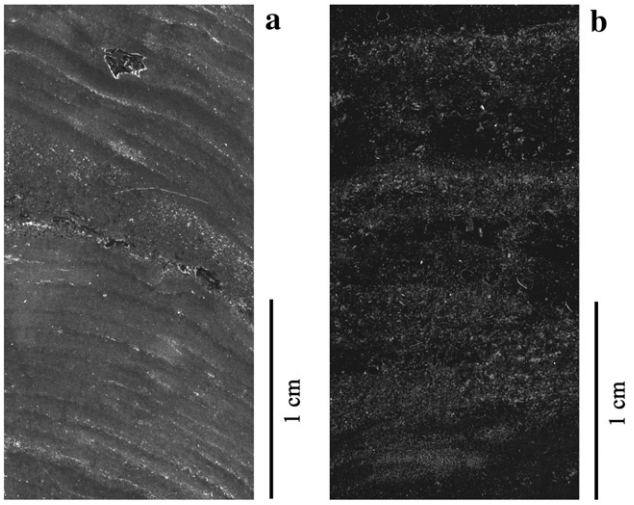

Fig. 3. a. A high-resolution scan of a polished sediment block with a turbidite across the center. The base of each varve can be identified by the layers of lighter colored sediments, b. A high-resolution scan of a polished sediment block with a turbidite characterized by cross-laminations.

used to estimate glacier high and low stands and therefore cool and/or wet and warm and/or dry climate phases, respectively. Centennial linear trends of $MAR_{LP}^{1/2}$ provided a record of glacier advances and retreats. These were used to infer transitions between warm and/or dry and cool and/or wet climates (i.e. cooling and/or wetting climate transitions) or between cool and/or wet and warm and/or dry climates (i.e. warming and/or drying climate transitions), respectively.

Centennial $MAR_{LP}^{1/2}$ anomalies and linear trends were compared to centennial turbidite frequencies (= # turbidites /100 years). The records were ranked in descending order according to the $MAR_{LP}^{1/2}$ values (either anomalies or linear trends) and smoothed with a 100 year moving average. A Pearson correlation coefficient ($r_{Pearson}$) and p value (corrected for autocorrelation; p_{corr}; Trenberth, 1984) was calculated to estimate the influence of long-term climate change (i.e. cool and/or wet phases, warm and/or dry phases, cooling and/or wetting climate transitions and warming and/or drying climate transitions) on turbidite frequency. These results were plotted and a linear regression tested whether the slope of the results were significantly different from zero. Following the same method, centennial average JJA temperatures from ca. 570 BC–AD 120 (quantitatively reconstructed from BSi flux and chironomids; Stewart et al., 2011) were used to compare centennial turbidite frequency to mean summer temperature.

To identify analogues for a warmer 21st century between ca. 570 BC–AD 120, 50 year windows with warming trends and averages exceeding the AD 1950–AD 2000 temperature values were identified. The frequency of turbidites during these 50 year windows was compared to the 1450 BC–AD 420 averages.

Additional statistical methods include changepoint analysis (constrained hierarchical clustering; Juggins, 2009; R Development Core Team, 2009), cross-correlation analysis and calculation of average and standard deviation.

4. Results and discussion

4.1. Lithology

Sediments throughout the section of interest consist of a light-colored silt basal layer (summer) capped by a dark clay layer (winter) (e.g. layered sediments above and below the turbidite in Fig. 3a). Couplets (approximate average thickness: 1.4 mm; maximum thickness: 3 mm; minimum thickness: 1 mm) are consistent with the varve descriptions of Ohlendorf et al. (1997) and Blass et al. (2007). Varves are interrupted by 85 (approximate average thickness: 8 mm; maximum thickness: 48 mm; minimum thickness: 1 mm) detrital-enriched and sandy deposits. In most cases, these consist of a thick deposit with coarsening upwards grainsize (i.e. inversely graded) which probably formed as flood conditions intensified and an upper deposit with fining upwards (i.e. normally graded) grainsize which likely formed as the flood waned (e.g. thick and sandy deposit in the center of Fig. 3a; Sturm and Matter, 1978; Mulder and Alexander, 2001). In other cases, these turbidites contain cross-laminations indicating a decreasing sediment load during waning of a flood (e.g. thick and sandy deposit composed of tilted sediment layers in Fig. 3b; Mulder and Alexander, 2001). These 85 deposits are thus interpreted to be flood-induced turbidites ('inundites').

4.2. Dating

Varve counts offer a chronology with inter-annual accuracy. The maximum difference between the varve counts when fixed at a turbidite around 4.4 m is 120 years. This difference could be related to falsely identifying laminations (Lamoureux and Bradley, 1996; Ojala, 2001).

Three calibrated radiocarbon dates (AD 16 ± 70, 52 BC ± 71 and 24 BC ± 82; Table 1), taken from terrestrial macrofossils in two nearby turbidites, are internally consistent (i.e. the difference between the number of varves and number of calibrated radiocarbon years between the two turbidites is equivalent). This suggests that terrestrial macrofossils within these two sampled turbidites are not reworked. These three calibrated radiocarbon dates and the varve counts are also in accordance with calibrated radiocarbon date 916 BC ± 85. Alternatively, terrestrial-macrofossil derived calibrated radiocarbon dates 3493 BC ± 128 and 1213 BC ± 157 are anomalously old and interpreted as reworked material (Wohlfarth et al., 1998). Therefore, only calibrated radiocarbon dates AD 16 ± 70, 52 BC ± 71, 24 BC ± 82 and 916 BC ± 85 are used in the final sediment chronology.

Table 1
Calibrated AMS radiocarbon dates (Intcal04.14) from Lake Silvaplana and sample characteristics. Sediment depth (m) with turbidites.

Code Poz-	Depth in core (m)	Material	Context	Sample mass (mg)	^{14}C age (±1σ) BP	Cal. ^{14}C age (±2σ) BC/AD
25246	~0.6	Bulk	Varves	16000	5950 ± 60	4848 BC ± 140
25245	~3.02	Bulk	Varves	58000	7890 ± 40	6995BC ± 31
25243	~2.2	Bulk	Varves	14000	6000 ± 40	4894 BC ± 100
25242	~1.7	Bulk	Varves	8000	7860 ± 50	6996BC ± 29
28061	~4.43	Needles	Turbidite	5.4	1985 ± 35	AD 16 ± 70
28062	~4.55	Needles	Turbidite	5	2020 ± 30	52 BC ± 71
28064	~4.55	Wood	Turbidite	7.2	2050 ± 30	24 BC ± 82
30292	~5.32	Needles	Turbidite	1	4665 ± 35	3493 BC ± 128
30293	~5.64	Needles	Turbidite	5	2765 ± 35	9 1 6 BC ± 85
30294	~5.64	Wood	Turbidite	4	2975 ± 35	1213 BC ± 157

The first series of varve counts fits through the four accepted calibrated radiocarbon dates better than the other two series. These varve counts, combined with the four calibrated radiocarbon dates, suggest that the entire sediment section spans approximately 1450 BC to AD 420 (±100) (Fig. 2). Additional details regarding the chronology can be found in Stewart et al. (2011).

4.3. Mass accumulation rate

MAR (ca.1450 BC to AD 420; Fig. 4a) averages 169 mg/cm^2/yr and has a standard deviation of 53 mg/cm^2/yr. Changepoints in MAR are found around 380 BC, AD 50 and AD 130.

The MAR record is consistent with an independent MAR record (MAR_{LN}) also from the distal region of Lake Silvaplana (Leemann and Niessen, 1994): following adjustment for a lag of 175 years (found through cross correlation), there is a significant ($p<0.01$) correlation between the two records and similar changepoints. This lag is consistent with the findings of Leemann and Niessen (1994) that the maximum difference between calibrated radiocarbon dates and varve counts in the MAR_{LN} chronology is 175 years.

As evident in Fig. 4a, MAR is below average between ca. 1450 BC and 900 BC with multi-decadal to centennial-scale oscillations. After 900 BC and until ca. AD 1, a millennial-scale increasing trend is super-imposed on these oscillations. After peaking at ~200 mg/cm^2/yr at ca. AD 1 MAR decreases to 100 mg/cm^2/yr where it remains until AD 100. This is followed by a rapid increase in MAR values. High MAR values persist for the remainder of the record.

MAR-inferred cool and/or wet and warm and/or dry phases (i.e. centennial anomalies in $MAR_{LP}^{1/2}$) and transitions between these phases (i.e. centennial trends in $MAR_{LP}^{1/2}$) are consistent with records of regional climate change from Central European lake levels (Magny, 2004), the Grosser Aletschgletscher (Swiss Alps; Holzhauser et al., 2005), glaciers in the Grimsel region (Swiss Alps; Joerin et al., 2006), the Pasterze Glacier (Austrian Alps; Nicolussi and Patzelt, 2000), the Gepatschferner (Austrian Alps; Nicolussi and Patzelt, 2001), silicious-based algae in sediments from Oberer Landschitzsee (Austrian Alps; Schmidt et al., 2007) and magnetic susceptibility in sediments from Lake Le Bourget (French Alps; Debret et al., 2010) (Figs. 4 d–f). Between ca. 1450 BC and 580 BC, negative centennial anomalies in $MAR_{LP}^{1/2}$ suggest a warm and/or dry climate. An increasing centennial linear trend in $MAR_{LP}^{1/2}$ from ca. 1340 BC coincides with elevated lake levels in Central Europe (Magny, 2004). This is followed by a decreasing centennial linear trend in $MAR_{LP}^{1/2}$ after ca. 1300 BC which is consistent with reduced length of the Grosser Aletschgletscher during the Bronze Age Optimum (Holzhauser et al., 2005). Another decreasing centennial linear trend in $MAR_{LP}^{1/2}$ after ca. 1020 BC (partly overlapping with a dendroclimatology and GRIP inferred warm and/or dry phase; Tinner et al., 2003) coincides with a retreat of the Pasterze Glacier (Nicolussi and Patzelt, 2000), glaciers in the Grimsel region (Joerin et al., 2006) and the establishment of trees on the forefield of Gepatschferner (Nicolussi and Patzelt, 2001). An increasing centennial linear trend in $MAR_{LP}^{1/2}$ after ca. 880 BC concurs with the flooding of lake-shore farmlands (Rychner et al., 1998; Tinner et al., 2003), higher lake levels in Central Europe (ca. 800 BC; Magny, 2004), cool spring temperatures at Oberer Landschitzsee (ca. 800 BC; Schmidt et al., 2007) and the Göschener cold phase I (approximately 1050 BC–350 BC; Furrer, 2001). There were also two advances of the Grosser Aletschgletscher (ca. 880 BC and ca. 700 BC; Holzhauser et al., 2005). Around 750 BC, a warming climate brought renewed farming north and south of the Alps and the transition from the Protogolasecca to Golasecca cultures (Tinner et al., 2003). Slightly warmer spring temperatures were also reconstructed from chrysophyte stomatocysts at Oberer Landschitzsee (Schmidt et al., 2007). This is reflected in negative $MAR_{LP}^{1/2}$ anomalies (ca. 750 BC–665 BC). Positive centennial anomalies of $MAR_{LP}^{1/2}$ around 580 BC to 400 BC coincide with elevated lake levels in Central Europe (Magny, 2004) and an extended Grosser Aletschgletscher (Holzhauser et al., 2005). The disappearance of farming locations north and south of the Alps and in the Upper Engadine may be associated with an increasing centennial linear trend in $MAR_{LP}^{1/2}$ ca. 400 BC to 265 BC (Gobet et al., 2003). This is followed by a brief decreasing centennial linear trend in $MAR_{LP}^{1/2}$ (ca. 265 BC–165 BC) which coincides with a shift from the Golasecca to La Tène cultures (Tinner et al., 2003), a continued retreat of the Grosser Aletschgletscher (Holzhauser et al., 2005), reduced Central European lake levels (Magny, 2004) and slightly higher spring temperatures recorded by chrysophyte stomatocysts in Oberer Landschitzsee (Schmidt et al., 2007). A shift to cooler conditions after ca. 210 BC is reflected in positive $MAR_{LP}^{1/2}$ anomalies (until approximately AD 50) and an increasing centennial linear trend in $MAR_{LP}^{1/2}$ from ca. 165 BC–85 BC. This roughly coincides with an influx of glacial sediments in Lake Le Bourget (Debret et al., 2010).

Increasing and decreasing centennial linear trends in $MAR_{LP}^{1/2}$ occur at ca. 85 BC to 30 BC and ca. 30 BC to AD 45, respectively. However, positive $MAR_{LP}^{1/2}$ anomalies persist. Alternatively, negative $MAR_{LP}^{1/2}$ anomalies are associated with a glacier retreat from ca. AD 45–AD 135 which is probably related to the Roman Age Optimum. During this time, agriculture intensified north and south of the Alps and in the Upper and Lower Engadine, and roads were constructed over open passes (Gobet et al., 2003; Tinner et al., 2003). Furthermore, chrysophyte stomatocysts in Oberer Landschitzsee recorded positive spring temperature anomalies (Schmidt et al., 2007), the Grosser Aletschgletscher reached a minimum extent (Holzhauser et al., 2005), the Pasterze Glacier retreated (Nicolussi and Patzelt, 2000), there were two retreats of glaciers in the Grimsel region and a retreat of glaciers in the Bernina region (Joerin et al., 2006), and trees were established on the forefield of Gepatschferner (Nicolussi and Patzelt, 2001). Around AD 135 to AD 335, increasing centennial linear trends in $MAR_{LP}^{1/2}$ occur. At ca. AD 310, the maximum positive $MAR_{LP}^{1/2}$ anomaly from ca. 1450 BC–AD 420 is achieved. This roughly coincided with an advance of the Grosser Aletschgletscher (Holzhauser et al., 2005), a rise in lake levels in Central Europe (Magny, 2004) and increased glacial sediments in Lake Le Bourget (Debret et al., 2010).

Slight variations among these natural archives (e.g. lake levels, glaciers) and $MAR_{LP}^{1/2}$ could be related to their response time to climate and their temporal resolutions. For example, chronological constraints on the Grosser Aletschgletscher curve between ca. 1450 BC to AD 420 are based on several fossil logs (Holzhauser et al., 2005).

4.4. Turbidite frequency

Turbidites (ca. 1450 BC to AD 420; Fig. 4b) have an average thickness of 8 mm and a standard deviation of 9 mm. The centennial frequency is reduced for the first four hundred years of record ($\leq$ ~0.04 per year; ca. 1450 BC–1050 BC; Fig. 4b). The centennial frequency is slightly elevated from ca. 1050 BC to 900 BC but returns to pre-1050 BC values from ca. 900 BC to 340 BC. Around 340 BC, turbidite frequencies up to 0.05 per year are reached. From approximately 95 BC to 65 BC centennial turbidite frequencies are 0.1 per year. Between ca. 65 BC and ca. AD 1, centennial turbidite frequency decreases. Centennial turbidite frequencies are slightly reduced from ca. AD 1 to AD 150. After AD 150, values rise and reach the record (ca. 1450 BC–AD 420) maximum at ca. AD 330.

4.5. The influence of long-term climate on turbidite frequency (ca. 1450 BC to AD 420)

In Fig. 5a, MAR-inferred phases of cool and/or wet and warm and/or dry climate are compared to centennial turbidite frequency. In Fig. 5b, MAR-inferred climate transitions (i.e. cooling and/or wetting and warming and/or drying) are compared to centennial turbidite frequency.

A significant positive correlation is found between $MAR_{LP}^{1/2}$ anomalies and turbidite frequency ($r_{Pearson} = 0.86$ and $p_{corr} < 0.01$) with a positive slope of the linear regression significantly different from zero. Negative

$MAR_{LP}^{1/2}$ anomalies coincide with turbidite frequencies around 0.02 turbidites per year. During positive $MAR_{LP}^{1/2}$ anomalies, turbidite frequencies increase almost linearly up to ca. 0.12 turbidites per year.

The rate of glacier advance or retreat (and therefore cooling and/or wetting and warming and/or drying climate transitions) has no significant correlation to turbidite frequency in our record.

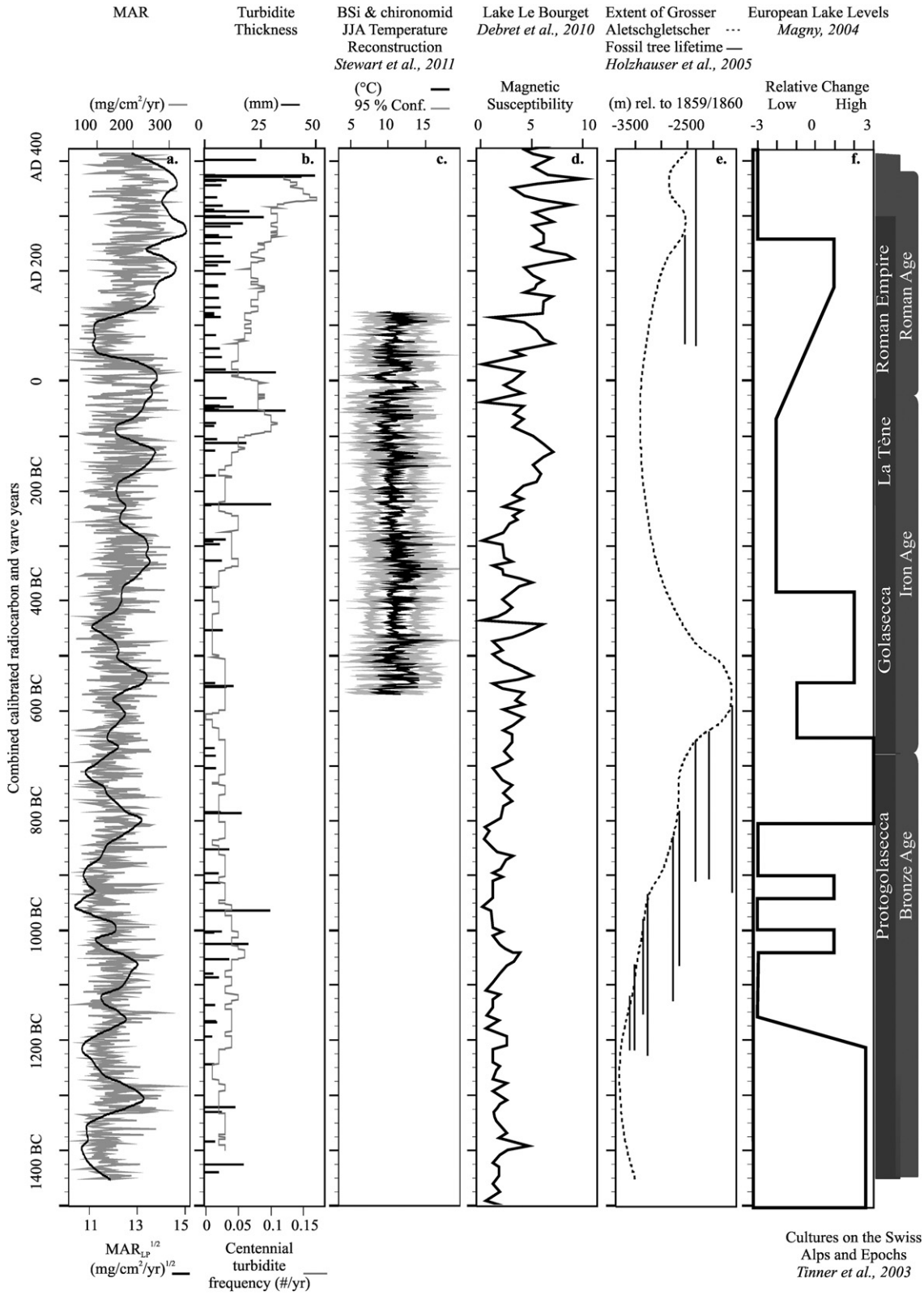

Fig. 4. a. Mass Accumulation Rate (MAR) overlain by $MAR_{LP}^{1/2}$, b. Turbidite thicknesses and the centennial turbidite frequency, c. Reconstructed June-July-August temperatures from Biogenic Silica (BSi) flux and chironomids (ca. 570 BC–AD 120) in the sediments of Lake Silvaplana (Stewart et al., 2011), d. The Lake Le Bourget magnetic susceptibility record (Debret et al., 2010), e. The Grosser Aletschgletscher extension curve (Holzhauser et al., 2005), f. Lake level fluctuations in Central Europe (Magny, 2004). Cultures on the Alps and associated Epochs are presented alongside the aforementioned figures (Tinner et al., 2003).

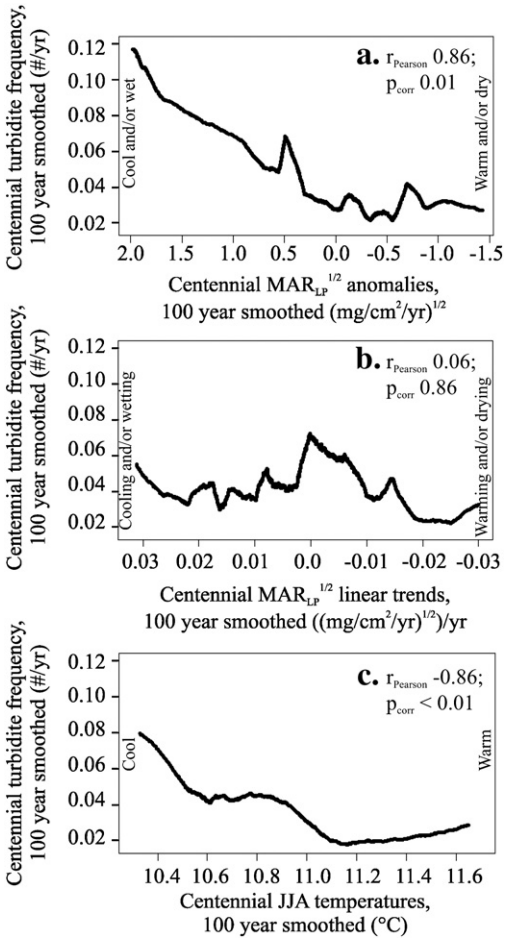

Fig. 5. a. Centennial anomalies in $MAR_{LP}^{1/2}$ and centennial turbidite frequency, ranked according to $MAR_{LP}^{1/2}$ and 100 year smoothed (ca. 1450 BC–AD 420), b. Centennial linear trends in $MAR_{LP}^{1/2}$ and centennial turbidite frequency, ranked according to $MAR_{LP}^{1/2}$ and 100 year smoothed (ca. 1450 BC–AD 420), c. Centennial JJA temperatures and centennial turbidite frequency, ranked according to JJA temperatures and 100 year smoothed (ca. 570 BC–AD 120).

4.6. The influence of JJA temperatures on turbidite frequency (ca. 570 BC to AD 120)

In Fig. 5c, average centennial JJA temperatures are compared to centennial turbidite frequency. This demonstrates a significant negative correlation between JJA temperatures and turbidite frequency ($r_{Pearson} = -0.86$ and $p_{corr} < 0.01$) with a negative slope of the linear regression that differs significantly from zero.

The decrease in turbidite frequency with increased average centennial JJA temperature includes several non-linearities. Turbidite frequency decreases with a warming climate until ca. 10.5 °C centennial mean JJA temperature. Turbidite frequency is unchanged from ca. 10.5 °C to 10.9 °C, and then decreases until 11.0 °C. Above centennial mean JJA temperatures of ca. 11.1 °C, the turbidite frequency is unchanged.

The overall behavior of turbidites with changing JJA temperatures is consistent with the relationship between $MAR_{LP}^{1/2}$ anomalies and turbidites. This suggests that especially cool and/or wet phases during the investigated time window (ca. 1450 BC–AD 420) and phases of cool JJA temperatures during the window ca. 570 BC–AD 120 favor an increase in the frequency of paleofloods. However, these relationships are not linear.

4.7. Turbidite frequency during windows with a trend and mean JJA temperature exceeding AD 1950–AD 2000

The relationship between turbidites and mean JJA temperatures was further investigated using 130 analogues (50 year windows) for a warmer 21st century in the Alps. These 50 year windows have an increasing trend and mean JJA temperature exceeding the Sils Maria AD 1950–AD 2000 reference period (Sils Maria AD 1950–AD 2000 JJA temperature trend = 0.02 °C/yr; average = 9.8 °C). Among these 130 windows, only 35 (27%) have a turbidite frequency exceeding the ca. 1450 BC–AD 420 50 year average (0.05 turbidites per year). Therefore, the frequency of turbidites (i.e. the frequency of paleofloods) is not enhanced during warmer periods of ca. 570 BC–AD 120.

Finally, more frequent turbidites occurred in Lake Silvaplana during the 20th century (Sils Maria AD 1900–AD 2000 JJA temperature average = 9.7 °C; Turbidite frequency = 0.2 turbidites per year; Blass, 2006) than during the warmer ca. 570 BC–AD 120 (JJA temperature average = 10.9 °C; Stewart et al., 2011).

As for most paleoenvironmental reconstructions, this study assumes that the relationship (e.g. between turbidite and extreme precipitation) during the observation period (i.e. Blass, 2006) is stable in time. For instance, we assume minimal channel migration on delta-fans located near the coring location. We are confident in the validity of these assumptions because Blass (2006) found that turbidites were a reliable indicator of extreme precipitation events during the last ca. 500 years despite changes in the catchment (e.g. glacier cover, land use) exceeding those from ca. 1450 BC–AD 420 (e.g. Gobet et al., 2003).

In sediments from Lake Silvaplana spanning AD 1177 to AD 2000, most turbidites are attributed to historical floods associated with severe summer-autumn precipitation (e.g. AD 1828, AD 1834, AD 1951, and AD 1987; Blass, 2006; Caviezel, 2007; Trachsel et al., 2010). To understand the atmospheric patterns responsible for these floods, we explored daily NCEP/NCAR reanalysis data (Kalnay et al., 1996; Kistler et al., 2001) of the mid-tropospheric geopotential height at 500 hPa (Z500) and Sea Level Pressure (SLP) during twelve severe summer-autumn precipitation events which formed turbidites in Lake Silvaplana between AD 1950 and AD 2000. We found strong negative anomalies of Z500 and SLP over Western Europe and the western Mediterranean (indicating a weak extension of the Azores high) allowing the passage of low pressure systems over Central Europe, stronger westerlies and favoring the advection of anomalous humid south-westerlies. This causes convective precipitation over the western Alps (Aux. 1, 2). During cooler summers, a higher frequency of turbidites (and therefore, paleofloods) is likely due to a strengthening of this atmospheric pattern.

5. Conclusions

Future climate scenarios project an increase in the frequency and severity of summer-autumn floods in Central Europe in a warmer climate. However, model projections and flood records (i.e. historical and instrumental) of the recent past have yet to reach a consensus (e.g. Christensen and Christensen, 2003; Mudelsee et al., 2003).

Insight into the relationship between floods and climate, under a wide range of climate variability in Central Europe from ca. 1450 BC to AD 420, can be found in the sediments of Lake Silvaplana (Upper Engadine, Switzerland). The frequency of local paleofloods can be reconstructed from turbidite frequency. Long-term cool and/or wet and warm and/or dry climate phases can be reconstructed from anomalies in low-frequency Mass Accumulation Rates (MAR). This is because low-frequency MAR reflects glacier length changes in the Swiss Alps and glacier lengths are a response to long-term climate conditions. Transitions between cool and/or wet and warm and/or dry climate phases can be inferred from centennial trends in low-frequency MAR. Furthermore, quantitative absolute June-July–August (JJA) temperatures reconstructed from Biogenic Silica (BSi) flux and

chironomids in the sediments of Lake Silvaplana are available from ca. 570 BC to AD 120 (Stewart et al., 2011).

Comparison of turbidite frequency to MAR-inferred climate phases (ca. 1450 BC–AD 420) and JJA temperatures (ca. 570 BC–AD 120) suggests an increase in the frequency of paleofloods during cool and/or wet climates and windows of cooler JJA temperatures. Specifically, the frequency of turbidites was reduced during warm and/or dry climates of ca. 1450 BC to AD 420. Following the transition to cool and/or wet climates, the frequency of turbidites increased. However, no discernable relationship between the rate of transition from warm and/or dry to cool and/or wet climate and turbidite could be found.

Increasing JJA temperatures from ca. 570 BC–AD 120 were matched by a decrease in the frequency of turbidites. However, the decrease was not linear. Finally, among 130 analogues (50 year windows) for warmer 21st century summers in the Alps, the average turbidite frequency was less than the ca. 1450 BC–AD 420 average.

The findings of this study suggest that the frequency of extreme summer-autumn precipitation events (i.e. flood events) and the associated atmospheric pattern in the Eastern Swiss Alps was not enhanced during warmer (or drier) periods of ca. 1450 BC–AD 420. Therefore, evidence could not be found that summer–autumn floods would increase in the Eastern Swiss Alps in a warmer climate of the 21st century. However, these findings need to be confirmed by independent (e.g. paleoflood and modeling) studies.

Supplementary materials related to this article can be found online at doi:10.1016/j.palaeo.2011.08.022.

Acknowledgements

This project was funded by the Swiss SNSF grant 'Enlarge II' (200021-116005/1). We appreciated access to the Mass Accumulation Rate record from Andreas Leemann and Frank Niessen, the magnetic susceptibility data-points from Maxime Debret, the turbidite record from Alex Blass and flood data from Peter Stucki. Statistical support came from Christian Kamenik and Mathias Trachsel. Modifications to the text came from Rixt de Jong, Isabelle Larocque, Jürg Luterbacher and Krystyna Saunders. The quality of the manuscript was greatly improved by suggestions from two reviewers and the journal Editor.

References

Abramoff, M.D., Magelhaes, P.J., Ram, S.J., 2004. Image processing with image. Journal Biophotonics International 11, 36–42.
AdS, 2004. Atlas der Schweiz – Interactive CD, version 2.0. Swiss Federal Office of Topography, Wabern.
Arnell, N., Liu, C., 2001. Hydrology and water resources. In: McCarthy, J.J., Canziani, O.F., Leary, N.A., Dokken, D.J., White, K.S. (Eds.), Climate Change 2001: Impacts, Adaptation and Vulnerability. Contribution of Working Group II to the Third Assessment Report of the Intergovernmental Panel on Climate Change. Cambridge University Press, Cambridge. Chapter 4.
Blass, A., 2006. Sediments of two high-altitude Swiss lakes as high-resolution late Holocene paleoclimate archives. Inauguraldissertation der Philosophisch-naturwissenschaftlichen Fakultät der Universität Bern.
Blass, A., Grosjean, M., Troxler, A., Sturm, M., 2007. How stable are twentieth-century calibration models? A high-resolution summer temperature reconstruction for the eastern Swiss Alps back to AD 1580 derived from proglacial varved sediments. The Holocene 17, 51–63.
Brázdil, R., Glaser, R., Pfister, C., Stangl, H., 2002. Floods in Europe — a look into the past. PAGES News 10, 21–23.
Caviezel, G., 2007. Hochwasser und ihre Bewältigung anhand des Beispiels Oberengadin 1750–1900. Unpublished Master's thesis, Universität Bern, 183 pp.
Christensen, J.H., Christensen, O.B., 2003. Climate modelling: severe summertime flooding in Europe. Nature 421, 805–806.
Debret, M., Chapron, E., Desmet, M., Rolland-Revel, M., Magand, O., Trentesaux, A., Bout-Roumazeille, V., Nomade, J., Arnaud, F., 2010. North western Alps Holocene paleohydrology recorded by flooding activity in Lake Le Bourget, France. Quaternary Science Reviews 29, 2185–2200.
Desloges, J.R., Gilbert, R., 1994. The record of extreme hydrological and geomorphological events inferred from glaciolacustrine sediments. In: Olive, L.J., Loughran, R.J., Kesby, J.A. (Eds.), Variability in Stream Erosion and Sediment Transport: International Association of Hydrological Sciences Publication No. 2 224, pp. 133–142.
Furrer, 2001. Alpine Vergletscherung vom letzten Hochglazial bis heute. Abhandlungen der Mathematisch-naturwissenschaftlichen Klasse, No. 3. Akademie der Wissenschaften und der Literatur, Mainz. 49 pp.
Gilbert, R., Desloges, J.R., 1987. Sediments of ice-dammed, self-draining Ape Lake, British Columbia. Canadian Journal of Earth Sciences 24, 1735–1747.
Gimmi, U., Luterbacher, J., Pfister, C., Wanner, H., 2007. A method to reconstruct long precipitation series using systematic descriptive observations in weather diaries: the example of the precipitation series for Bern, Switzerland (1760–2003). Theoretical and Applied Climatology 87, 185–199.
Gobet, E., Tinner, W., Hochuli, P.A., van Leeuwen, J.F.N., Ammann, B., 2003. Middle to Late Holocene vegetation history of the Upper Engadine (Swiss Alps): the role of man and fire. Vegetation Historical Archaeobotany 12, 143–163.
Holzhauser, H., Magny, M., Zumbühl, H.J., 2005. Glacier and lake-level variations in west-central Europe over the last 3500 years. The Holocene 15, 789–801.
Joerin, U.E., Stocker, T.F., Schlüchter, C., 2006. Multicentury glacier fluctuations in the Swiss Alps during the Holocene. The Holocene 16, 697–704.
Joerin, U.E., Stocker, T.F., Schlüchter, C., 2006. Multicentury glacier fluctuations in the Swiss Alps during the Holocene. The Holocene 16, 697–704.
Kääb, A., Paul, F., Maisch, M., Hoelzle, M., Haeberli, W., 2002. The new remote-sensing derived Swiss glacier inventory: II. First Results. Annals of Glaciology 34, 362–366.
Kalnay, E., Kanamitsu, M., Kistler, R., Collins, W., Deaven, D., Gandin, L., Iredell, M., Saha, S., White, G., Woollen, J., Zhu, Y., Chelliah, M., Ebisuzaki, W., Higgins, W., Janowiak, J., Mo, K.C., Ropelewski, C., Wang, J., Leetmaa, A., Reynolds, R., Jenne, R., Joseph, D., 1996. The NMC/NCAR 40-Year Reanalysis Project. Bulletin of the American Meteorological Society 77, 437–471.
Kistler, R., Kalnay, E., Collins, W., Saha, S., White, G., Woollen, J., Chelliah, M., Ebisuzaki, W., Kanamitsu, M., Kousky, V., van den Dool, H., Jenne, R., Fiorino, M., 2001. The NCEP-NCAR 50-year reanalysis: monthly means CD-ROM and documentation. Bulletin of the American Meteorological Society 82, 247–267.
Knighton, D., 1998. Fluvial Forms and Processes: A New Perspective. Oxford University Press, London. 383 pp.
Kundzewicz, Z.W., Ulbrich, U., Brücher, T., Graczyk, D., Krüger, A., Leckebusch, G.C., Menzel, L., Pińskwar, I., Radziejewski, M., Szwed, M., 2005. Summer floods in Central Europe — climate change track? Natural Hazards 36, 165–189.
Lamoureux, S., Bradley, R.S., 1996. A late Holocene varved sediment record of environmental change from northern Ellesmere Island, Canada. Journal of Paleolimnology 16, 239–255.
Leemann, A., Niessen, F., 1994. Holocene glacial activity and climatic variations in the Swiss Alps: reconstructing a continuous record from proglacial lake sediments. The Holocene 4, 259–268.
LIMNEX, 1994. Gewässerzustand und Gewässerschutzmassnahmen im Oberengadin. Bericht zuhanden des Amtes für Umweltschutz, Kanton Graubünden. 75 pp.
Magny, M., 2004. Holocene climatic variability as reflected by mid-European lake-level fluctuations and its probable impact on prehistoric human settlements. Quaternary International 113, 65–79.
Maisch, M., 1992. Die Gletscher Graubündens. Habil. Schrift Geographisches Institut Universität Zürich. Teil A und B. Physische Geographie, Vol. 33. 428 pp.
Mappad Free Software, 1996. http://www.ngdc.noaa.gov/paleo/paleo.html (accessed 2010).
MeteoSchweiz, 2010. http://www.meteoschweiz.admin.ch/web/de/klima/klima_heute/jahresverlaeufe_nbcn/Segl_Maria.html (accessed 2010).
Mudelsee, M., Börngen, M., Tetzlaff, G., Grünewald, U., 2003. No upward trends in the occurrence of extreme floods in central Europe. Nature 425, 166–169.
Mudelsee, M., Börngen, M., Tetzlaff, G., Grünewald, U., 2004. Extreme floods in central Europe over the past 500 years: role of cyclone pathway "Zugstrasse Vb. Journal of Geophysical Research 109, D23101.
Mulder, T., Alexander, J., 2001. The physical character of subaqueous sedimentary density flows and their deposits. Sedimentology 48, 269–299.
Nicolussi, K., Patzelt, G., 2000. Discovery of early-Holocene wood and peat on the forefield of the Pasterze Glacier, Eastern Alps, Austria. The Holocene 10, 191–199.
Nicolussi, K., Patzelt, G., 2001. Untersuchungen zur holozänen Gletscherentwicklung von Pasterze und Gepatschferner (Ostalpen). Zeitschrift für Gletscherkunde und Glazialgeologie 36, 1–87.
Nussbaumer, S.U., Steinhilber, F., Trachsel, M., Breitenmoser, P., Beer, J., Blass, A., Grosjean, M., Hafner, A., Holzhauser, H., Wanner, H., Zumbühl, H.J., 2011. Alpine climate during the Holocene: a comparison between records of glaciers, lake sediments and solar activity. Journal of Quaternary Science 26. doi:10.1002/jqs.1495.
Ohlendorf, C., 1999. High Alpine lake sediments as chronicles for regional glacier and climate history in the Upper Engadine, southeastern Switzerland. Berichte aus der Geowissenschaft Shaker Verlag, Aachen. 203 pp.
Ohlendorf, C., Niessen, F., Weissert, H., 1997. Glacial varve thickness and 127 years of instrumental climate data: a comparison. Climatic Change 36, 391–411.
Ojala, A., 2001. Varved Lake Sediments in Southern and Central Finland: Long varve chronologies as a basis for Holocene palaeoenvironmental reconstructions. Academic Dissertation, Geological Survey of Finland, Espoo, 41 pp.
Paul, F., 2007. The new Swiss glacier inventory 2000 — application of remote sensing and GIS. Physische Geographie, Vol. 52. Geographisches Insitut der Universität Zürich, Zürich. 210 pp.
Paul, F., Kääb, A., Maisch, M., Kellenberger, T., Haeberli, W., 2002. The new remote-sensing derived Swiss glacier inventory: I Methods. Annals of Glaciology 34, 355–361.
Pauling, A., Luterbacher, J., Casty, C., Wanner, H., 2006. Five hundred years of gridded high-resolution precipitation reconstructions over Europe and the connection to large-scale circulation. Climate Dynamics 26, 387–405.
Pfister, C., Weingartner, R., Luterbacher, J., 2006. Hydrological winter droughts over the last 450 years in the Upper Rhine basin: a methodological approach. Hydrological Sciences Journal 51, 966–985.

R Development Core Team, 2009. R: A language and environment for statistical computing. R Foundation for Statistical Computing, Vienna, Austria.

Reimer, P.J., Baillie, M.G.L., Bard, E., Bayliss, A., Beck, J.W., Bertrand, C., Blackwell, P.G., Buck, C.E., Burr, G., Cutler, K.B., Damon, P.E., Edwards, R.L., Fairbanks, R.G., Friedrich, M., Guilderson, T.P., Hughen, K.A., Kromer, B., McCormac, F.G., Manning, S., Bronk Ramsey, C., Reimer, R.W., Remmele, S., Southon, J.R., Stuiver, M., Talamo, S., Taylor, F.W., van der Plicht, J., Weyhenmeyer, C.E., 2004. IntCal04 Terrestrial Radiocarbon Age Calibration, 0–26 cal kyr BP. Radiocarbon 46, 1029–1058.

Rychner, V., Bolliger Schreyer, S., Carazzetti, R., David-Elbiali, M., Hafner, A., Hochuli, S., Janke, R., Rageth, J., Seifert, M., 1998. Geschichte und Kulturen der Bronzezeit in der Schweiz. In: Hochuli, S., Niffeler, U., Rychner, V. (Eds.), Die Schweiz vom Paläolithikum bis zum frühen Mittelalter – Bronzezeit. Verlag Schweizerische Gesellschaft für Ur- und Frühgeschichte, Basel, pp. 103–133.

Schmidt, R., Kamenik, C., Roth, M., 2007. Siliceous algae-based seasonal temperature inference and indicator pollen tracking ca. 4,000 years of climate/land use dependency in the southern Austrian Alps. Journal of Paleolimnology 38, 541–554.

Schmocker-Fackel, P., Naef, F., 2010. Changes in flood frequencies in Switzerland since 1500. Hydrology and Earth System Sciences 14, 1581–1594.

Steiner, D., Walter, A., Zumbühl, H.J., 2005. The application of a non-linear back-propagation neural network to study the mass balance of Grosse Aletschgletscher, Switzerland. Journal of Glaciology 51, 313–323.

Stewart, M., Larocque-Tobler, I., Grosjean, M., 2011. Quantitative inter-annual and decadal summer temperature variability 570 BC–AD 120 (Iron Age–Roman Period) reconstructed from the varved sediments of Lake Silvaplana, Switzerland. Journal of Quaternary Science 26, 491–501.

Sturm, M., Matter, A., 1978. Turbidites and varves in Lake Brienz (Switzerland): deposition of clastic detritus by density currents. In: Matter, A., Tucker, M.E. (Eds.), Modern and Ancient Lake Sediments. Special Publications International Association of Sedimentologists. Blackwell Scientific Publications, Oxford, pp. 147–168.

Tinner, W., Lotter, A.F., Ammann, B., Conedera, M., Hubschmid, P., van Leeuwen, J.F.N., Wehrli, M., 2003. Climatic change and contemporaneous land-use phases north and south of the Alps 2300 BC to 800 AD. Quaternary Science Reviews 22, 1447–1460.

Trachsel, M., Eggenberger, U., Grosjean, M., Blass, A., Sturm, M., 2008. Mineralogy-based quantitative precipitation and temperature reconstructions from annually laminated lake sediments (Swiss Alps) since AD 1580. Geophysical Research Letters 35, L13707.

Trachsel, M., Grosjean, M., Larocque-Tobler, I., Schwikowski, M., Blass, A., Sturm, M., 2010. Quantitative summer temperature reconstruction derived from combined biogenic Si and chironomid record from varved sediments of Lake Silvaplana (south-eastern Swiss Alps) back to AD 1177. Quaternary Science Reviews 29, 2719–2730.

Trenberth, K.E., 1984. Some effects of finite sample size and persistence on meteorological statistics. Part I: Autocorrelation. Monthly Weather Review 112, 2359–2368.

Trenberth, K.E., Jones, P.D., Ambenje, P., Bojariu, R., Easterling, D., Klein Tank, A., Parker, D., Rahimzadeh, F., Renwick, J.A., Rusticucci, M., Soden, B., Zhai, P., 2007. Observations: Surface and Atmospheric Climate Change. In: Solomon, S., Qin, D., Manning, M., Chen, Z., Marquis, M.C., Averyt, K.B., Tignor, M., Miller, H.L. (Eds.), Climate Change 2007. The Physical Science Basis. Contribution of WG 1 to the Fourth Assessment Report of the Intergovernmental Panel on Climate Change. Cambridge University Press, Cambridge.

Wohlfarth, B., Skog, G., Possnert, G., Homquist, B., 1998. Pitfalls in the AMS radiocarbon-dating of terrestrial macrofossils. Journal of Quaternary Science 13, 137–145.

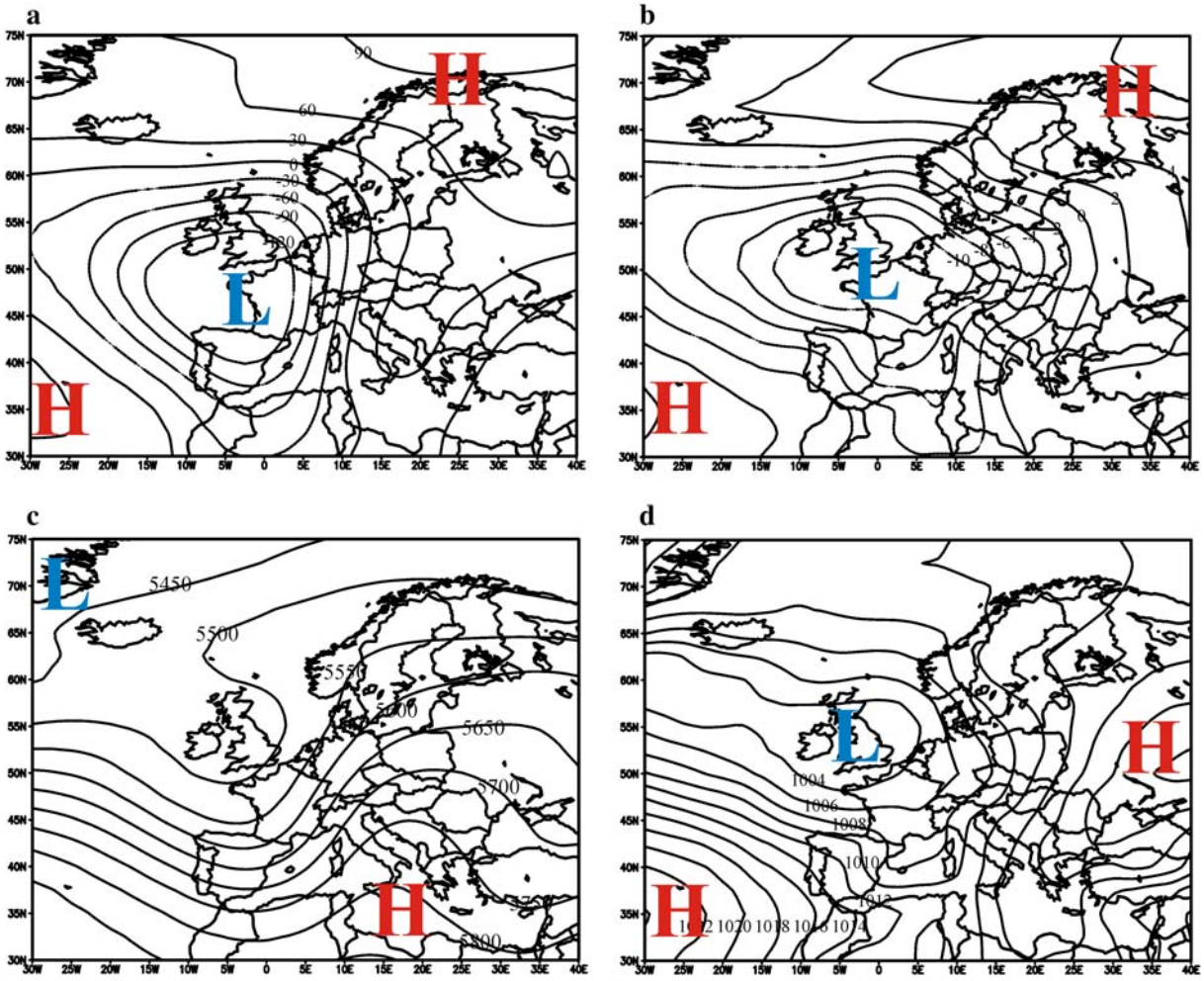

Aux. Fig. 1. a., b. Composite anomalies and c., d. composite means (both in respect to the AD 1968–AD 1996 climatology) for twelve summer-autumn precipitation events responsible for turbidites in Lake Silvaplana between AD 1950 and AD 2000 (11/08/1951, 8/21/1954, 6/7/1955, 9/20/1956, 11/6/1957, 11/9/1961, 6/23/1978, 7/18/1987, 8/24/1987, 9/20/1999, 10/13/2000 and 10/14/2000) from NCEP/NCAR Reanalysis (Kalnay et al., 1996 and Kistler et al., 2001). H and L denote the centers of positive and negative Z500 and SLP anomalies and means, respectively.

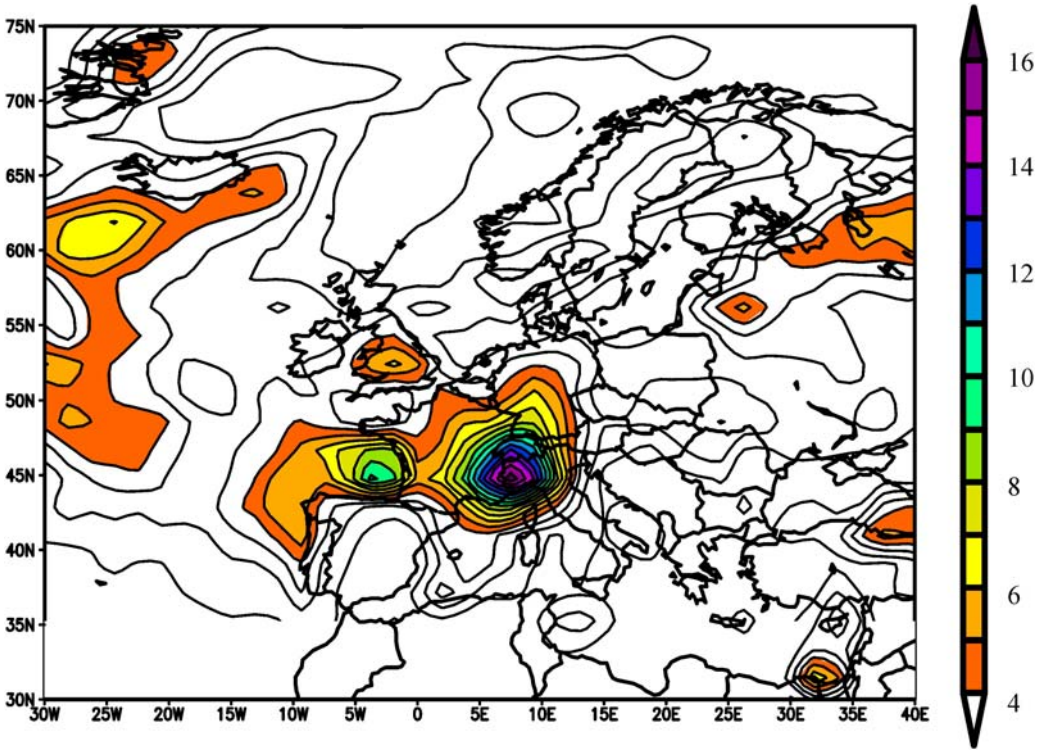

Aux. Fig. 2. Mean daily precipitation sums (mm/day) during the twelve summer-autumn precipitation events which produced turbidites in Lake Silvaplana between AD 1950 and AD 2000 from NCEP/NCAR Reanalysis (Kalnay et al., 1996 and Kistler et al., 2001).